

Dislocation dynamics. I. A proposed methodology for deformation micromechanics

R. J. Amodeo* and N. M. Ghoniem

*Mechanical, Aerospace and Nuclear Engineering Department, University of California, Los Angeles,
Los Angeles, California 90024*

(Received 10 July 1989)

A new methodology in computational micromechanics, dislocation dynamics (DD), is introduced. Dislocation dynamics is developed for examining the dynamic behavior of dislocation distributions in solid materials. Under conditions of externally applied stress, dislocations exhibit glide with a velocity proportional to a power of the applied stress σ^m and climb motion with a velocity that is a function of the applied stress and temperature. These motions result from long-range force fields, comprising both externally applied stress and long-range interactions between individual dislocations. Short-range reactions are represented as discrete events. The DD methodology is to be differentiated from particle methods in statistical mechanics (e.g., molecular dynamics and the Monte Carlo method) in two respects. First, DD is developed to study the dynamical behavior of "defects" in the solid. Generally, the density of defects is less than that of the particles that make up the solid. Second, the small number of dislocations allows for a complete dynamical representation of the evolution of dislocations in the material medium without the requirement of statistical averaging. The purpose of the DD methodology is to bridge the gap between experimentally observed phenomena and theoretical descriptions of dislocation aggregates, particularly the evolution of self-organized dislocation structures under temperature, stress, and irradiation conditions.

I. INTRODUCTION

Dynamical methods were formulated to predict the time-dependent trajectories of a number of interacting particles. The term molecular dynamics (MD) has been used to describe the early versions of such calculations that were applied to the study of the motion of molecules in a fluid. Alder and Wainwright¹ were the first to perform MD calculations using discrete potentials. In 1964, Rahman² made the first MD simulations of fluids with continuous potentials. Verlet³ made significant contributions to further application and understanding of the MD process. In 1980, Andersen⁴ proposed a mixed Monte Carlo (MC)-MD algorithm for performing isothermal simulations where stochastic collisions from a heat bath are treated in accord with the MC process. A similar approach for a many-body system has been suggested by Abraham,⁵ where the equations of motion (EOM's) are solved considering the stochastic component due to Brownian motion.

Although it is impractical to simulate the microscopic dynamics of atoms or molecules within a solid lattice containing a dilute concentration of defects, we can simulate the inverse problem of the motion of defects within the solid. Dislocations are line defects within a solid which, although existing on a microscopic level, can produce macroscopic changes in the properties of the solid medium. A dislocation is a local discontinuity in an otherwise perfect lattice structure. In a three-dimensional (3D) array of atoms within a crystal, removing a half plane of atoms within the crystal leads to a local singularity called a dislocation. This produces a distortion of the crystal leading to a long-range elastic field.

Dislocations only exhibit macroscopic forces by the

transference of elastic energy through the solid medium. In this sense a distinct difference can be drawn between defect (dislocation) dynamics (DD) and MD. In the latter, the particles constitute the medium and interaction primarily occurs through nearest-neighbor forces (gases) or local bonding (liquid). In the former, the particles are singularities (defects) which are distinct from the medium. The solid is almost like an ether through which the dislocation particles propagate.

Here we propose a new simulation methodology, DD, applicable to bulk solid systems. The system of dislocations is treated as a collection of vector particles, and the simulation is enacted through application of a new general methodology, vector particle dynamics. In Sec. II we describe the physics defining the collective dynamical interaction between components of a large dislocation system. Section III is a description of the computer methodology which is characteristic of DD simulations and sample results. Section IV of this paper is a discussion of the main features of the DD methodology, and includes a comparison with traditional MD methodology. In a companion paper, "Dislocation Dynamics. II." we present applications of the methodology to the study of the formation of planar dislocation arrays, persistent slip bands (PSB's), and dislocation cells.

II. INTERACTION PHYSICS

A. Dislocation motion in solids

Dislocation motion in the glide plane (glide) is in the direction of the Burgers vector for edge dislocations and orthogonal to the Burgers vector for screw dislocations. In addition, screw dislocations can cross slip from one

glide plane to another. Climb is the motion of a dislocation perpendicular to the glide plane.

1. Glide velocity

The glide velocity of a dislocation is attributed to the action of an effective force applied in the glide direction of the dislocation.⁶ At lower temperatures, obstacles controlling glide are overcome by stress-assisted thermal activation. At higher temperatures, the obstacles controlling glide are athermal⁷ causing the flow stress to be approximately constant with temperature. The glide velocity is generally given by⁸

$$v_g = M_g F_g, \quad (1)$$

where M_g is the mobility for dislocation glide and F_g is equal to the net force in the glide direction.

The glide mobility is characterized by the diffusive properties of the material⁹ and is governed by the diffusion of dislocations through the obstacles with the shortest spacing:

$$M_g = D_s b / kT, \quad (2)$$

where D_s is the self-diffusion coefficient, b is the magnitude of the Burgers vector, k is the Boltzmann constant, and T is absolute temperature.

This linear dependence of velocity on stress is valid only for a limited range of applied stress. It has been found experimentally,¹⁰⁻¹² over a wide range of applied stress, that the relationship between velocity and stress is nonlinear. This dependence is given by the following expression:¹³

$$v_g = v_s (\tau_{\text{eff}} / \tau_s)^m, \quad (3)$$

where v_s is the shear wave velocity, τ_{eff} the effective shear stress on dislocations, τ_s the material stress constant, and m the stress exponent.

Three different regions of the stress dependence described by Eq. (3) have been found for many metals.¹⁴ The stress exponents for these regions are $m_{\text{I}} > 1$, $m_{\text{II}} = 1$, and $m_{\text{III}} < 1$, with the maximum velocity limited by the shear wave velocity. The velocity-stress relationship for iron has been determined for a wide range of conditions of stress and temperature.¹¹ We can characterize the velocity-stress relationship for iron by three separate regions of differing values of τ_s and exponent m . It is found that the effective material stress constant can be related to the absolute temperature T and the shear modulus μ of the material by the following expression:

$$\tau_s = C \mu e^{E/mkT}. \quad (4)$$

Table I is a compilation of the constants C and the stress exponent m for iron for the three different velocity-stress regions. The value of the characteristic energy E in Eq. (4) is 0.4876 eV.

This stress dependence is the direct effect of stress on the movement of a single dislocation in the system, without regard to the presence of other obstacles (including other dislocations) which can drastically alter the stress dependence. The effect of other dislocations and

TABLE I. Coefficients for the glide velocity-stress relationship in iron.

Region	m	C
I	35.0	1.87×10^{-3}
II	1.0	4.118×10^{-9}
III	0.672	5.35×10^{-13}

obstacles is evaluated by the overall local stress field determined by the short- and long-range interactions with all other dislocations. The internal stress on a dislocation is therefore a result of the integrated system effect and not a predetermined material parameter.

2. Climb velocity

At higher temperatures, the process of climb constitutes the dominant mode of dislocation motion. Dislocation climb is thermally activated and is considered a stress-assisted thermal process. It is therefore dependent upon the diffusive properties of the material, particularly the diffusion of vacancies to the dislocation core. A phenomenological expression for the dislocation climb velocity is given by¹⁵

$$v_c = v_0 (\tau_a / \mu), \quad (5)$$

where τ_a is the applied shear stress and v_0 is a characteristic climb velocity given by

$$v_0 = A (D_s / b) (\mu \Omega / kT) c_j (\chi / \mu b)^2, \quad (6)$$

where A is the constant on the order 1000, Ω is the atomic volume, c_j is the concentration of jogs, and χ is the stacking fault energy.

B. Long-range forces

Outside a core radius of about five Burgers vectors from a dislocation, the force exerted by a dislocation on another dislocation is inversely proportional to the separation distance. This represents the long-range force of a dislocation, because the local distortion of the lattice is negligible compared with the elastic straining of the material at large distances from the dislocation core. For these long-range reactions, the property of linearity holds and the total force on a given dislocation can be computed by summing the individual long-range forces resulting from all other dislocations. The following is a discussion of the methodologies used to define the long-range interaction between elements in a system of dislocations.

1. General methodology

Dislocations exhibit glide in different slip planes and each glide direction may represent a local coordinate system. For convenience, we refer to them as reference dislocations R_r (dislocations for which forces are computed) and test dislocations R_t (dislocations which exhibit the long-range forces). Figure 1 is an illustration of the interaction of an arbitrary test dislocation with the reference dislocation. In order to compute the forces between a test dislocation in one system and a reference dislocation

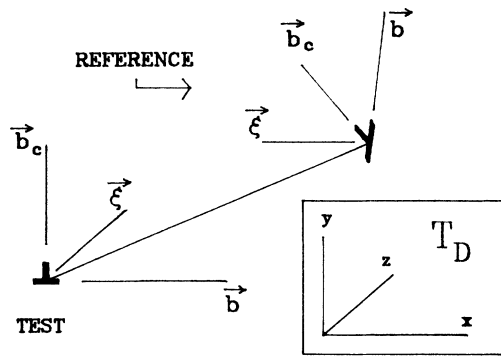


FIG. 1. General coordinate convention for two interacting dislocations.

tion in another system, a conventional coordinate system must be chosen to correctly implement the transformations. The force from the test dislocation is rotationally transformed into the coordinate system of the reference dislocation (the abscissa is represented by the direction of glide and the ordinate is represented by the direction of climb). Another test dislocation is chosen, its forces on the reference dislocation are computed, and the resultant forces are added to the total force. These forces are summed up linearly and then the velocity of the dislocation based on this total force is computed.

For the general methodology, the x direction represents the dislocation Burgers vector \mathbf{b} , the y direction represents the dislocation climb vector \mathbf{b}_c , and the z direction represents the sense vector of the dislocation ξ . This coordinate convention is graphically represented in Fig. 1. If, for example, the system consists of three coplanar dislocations, all traveling on different (111) glide planes, one of the dislocations represents the primary dislocation. The three-dimensional (3D) characteristics of this dislocation can then be expressed in general terms as a tensor which consists of components

$$\underline{T}_D = \begin{pmatrix} \mathbf{b} \\ \mathbf{b}_c \\ \xi \end{pmatrix} = \begin{pmatrix} b_x & b_y & b_z \\ b_{cx} & b_{cy} & b_{cz} \\ \xi_x & \xi_y & \xi_z \end{pmatrix}. \quad (7)$$

This can be considered the dislocation tensor (DT). By convention, the DT of a primary dislocation is given by the identity matrix. All other dislocation types will have DT's which are necessarily different from the primary DT.

The force from a test dislocation on a reference dislocation is given by the Peach-Koehler equation¹⁶

$$\mathbf{F} = (\mathbf{b} \cdot \underline{\Sigma}) \xi. \quad (8)$$

The stress tensor $\underline{\Sigma}$ is determined by transforming the stress tensor of a test dislocation $\underline{\Sigma}_t$ into the reference coordinate system. The stress tensor $\underline{\Sigma}_t$ of an arbitrary test dislocation is given by¹⁷

$$\underline{\Sigma}_t = \begin{pmatrix} \sigma_{xx} & \sigma_{xy} & \sigma_{xz} \\ \sigma_{yx} & \sigma_{yy} & \sigma_{yz} \\ \sigma_{zx} & \sigma_{zy} & \sigma_{zz} \end{pmatrix}, \quad (9)$$

where, in Cartesian coordinates

$$\begin{aligned} \sigma_{xx} &= -\frac{\mu b}{2\pi(1-\nu)} \left[\frac{y(3x^2+y^2)}{(x^2+y^2)^2} \right], \\ \sigma_{xy} &= \frac{\mu b}{2\pi(1-\nu)} \left[\frac{x(x^2-y^2)}{(x^2+y^2)^2} \right], \\ \sigma_{xz} &= 0, \\ \sigma_{yx} &= \sigma_{xy}, \\ \sigma_{yy} &= \frac{\mu b}{2\pi(1-\nu)} \left[\frac{y(x^2-y^2)}{(x^2+y^2)^2} \right], \\ \sigma_{yx} &= 0, \\ \sigma_{zx} &= 0, \\ \sigma_{zy} &= 0, \\ \sigma_{zz} &= -\frac{\mu b}{\pi(1-\nu)} \frac{y}{x^2+y^2}, \end{aligned}$$

for edge dislocations with the sense direction vector ξ coincident with the z axis, and

$$\begin{aligned} \sigma_{xz} &= -\frac{\mu b}{2\pi} \frac{y}{x^2+y^2}, \\ \sigma_{yz} &= -\frac{\mu b}{2\pi} \frac{x}{x^2+y^2}, \\ \sigma_{xx} &= \sigma_{xy} = \sigma_{yx} = \sigma_{yy} = \sigma_{zz} = 0, \end{aligned}$$

for screw dislocations with ξ lying along the z axis. ν is Poisson's ratio.

The rotational transform between two coordinate systems i and j is given by

$$\underline{T}_{rot} = \underline{T}_{ij} = [\underline{T}_{Di}] \cdot [\underline{T}_{Dj}]. \quad (10)$$

If system j is the primary coordinate system, the transformation becomes

$$\underline{T}_{rot} = \underline{T}_i = [\underline{T}_{Di}]. \quad (11)$$

Transforming the components of $\underline{\Sigma}_t$ (i.e., σ_{ij} ; $i, j \in x, y, z$) into the primary coordinate system is accomplished by the following operation:

$$\underline{\Sigma} = \underline{T}_{rot} \cdot \underline{T}_{rot} \cdot \underline{\Sigma}_t = \sum_{l=x}^z \sum_{m=x}^z T_{il} T_{jm} \sigma_{lm}. \quad (12)$$

A total long-range stress tensor is computed by summing up contributions from all dislocations given by Eq. (12) in addition to the applied stress. An effective stress tensor is defined as this sum of applied and internal stress minus the friction stress. the resulting force (Peach-Koehler) is obtained by applying Eq. (8) to the effective stress tensor. the resulting force components can be expressed as

$$\mathbf{F} = \begin{pmatrix} F_g \\ F_c \\ F_\xi \end{pmatrix}, \quad (13)$$

where F_g and F_c are the glide and climb force, respective-

ly, and F_ξ is the force along dislocation sense vector ξ . All are in the reference dislocation's coordinate system.

The glide velocity can then be calculated using the velocity-stress relationship [Eq. (3)] and the climb velocity is determined by using Eqs. (5) and (6). The velocity vector \mathbf{v}_r of the reference dislocation is then given by

$$\mathbf{v}_r = \begin{pmatrix} v_g \\ v_c \\ 0 \end{pmatrix}. \quad (14)$$

The velocity component along ξ is assumed to be zero since the dislocation has no mobility along ξ . The resulting displacement of the reference dislocation $\Delta \mathbf{r}_r$ is obtained by explicit integration of Eq. (14):

$$\Delta \mathbf{r}_r = \Delta t \mathbf{v}_r, \quad (15)$$

where the time step Δt is chosen to satisfy local error control criteria, as will be shown in Sec. III. This displacement vector must be transformed into the global dislocation coordinate system by projecting the components of the displacement onto the global system by the dislocation tensor:

$$\Delta \mathbf{r} = \Delta \mathbf{r}_r \cdot \mathbf{T}_D. \quad (16)$$

Finally, the new position \mathbf{r}_k is computed by adding the displacement $\Delta \mathbf{r}$ to the previous position of the dislocation \mathbf{r}_{k-1} :

$$\mathbf{r}_k = \mathbf{r}_{k-1} + \Delta \mathbf{r}. \quad (17)$$

Although the treatment of long-range forces can be determined through the use of Eqs. (7)–(17), a practical 3D model would entail considerable computational difficulties. One of the major aspects of a 3D model is the accurate representation of dislocation curvature as the dynamics progress in time. A simpler 2D model will be presented in the remainder of this paper. Applications of this 2D model will be given in paper II.

2. Parallel dislocations

If two dislocations are parallel, we can construct simple solutions to the above equations by eliminating the dislocation sense vector direction, and solving the equations in cylindrical coordinates. Figure 2 illustrates the coordinate system chosen for this special, yet important, case. In the figure, θ is the angle of the reference dislocation with respect to the test dislocation, $\alpha_{t,r}$ are the glide direction angles of the test and reference dislocations with respect to the global coordinate system, and γ is the relative angle between the two dislocations.

Application of Eq. (8) in cylindrical coordinates results in the following expressions of stress on the reference dislocation from the test dislocation in the test coordinate system:

$$\underline{\Sigma}_t = \begin{pmatrix} \sigma_{rr} & \sigma_{r\theta} \\ \sigma_{\theta r} & \sigma_{\theta\theta} \end{pmatrix}, \quad (18)$$

where $\sigma_{rr} = \sigma_{\theta\theta} = -K(\sin\theta/R)$, $\sigma_{r\theta} = \sigma_{\theta r} = K(\cos\theta/R)$,

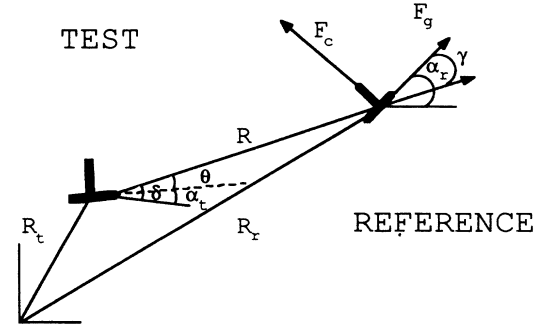


FIG. 2. Parallel dislocation coordinate convections.

$K = \mu b / 2\pi(1 - \nu)$, and R is the radial distance away from the dislocation.

The rotational transform, which rotates the stress tensor into the reference dislocation's coordinate system, is given by

$$\mathbf{T}_{\text{rot}} = \begin{pmatrix} \cos\gamma & \sin\gamma \\ -\sin\gamma & \cos\gamma \end{pmatrix}, \quad (19)$$

and therefore the stress in the reference dislocation's system is given by

$$\underline{\Sigma} = \mathbf{T}_{\text{rot}} \cdot \mathbf{T}_{\text{rot}} \cdot \underline{\Sigma}_t = \begin{pmatrix} \sigma_{11} & \sigma_{12} \\ \sigma_{21} & \sigma_{22} \end{pmatrix}, \quad (20)$$

where

$$\sigma_{11} = -K(\sin\theta - \sin 2\gamma \cos\theta) / R,$$

$$\sigma_{12} = K \cos\theta \cos 2\gamma / R = \sigma_{21},$$

$$\sigma_{22} = -K(\sin\theta + \sin 2\gamma \cos\theta) / R.$$

Substituting Eq. (20) into Eq. (8), we arrive at the expression for force components on a dislocation, which are given by the climb and glide components per unit length L , as

$$\frac{F_c}{L} = \frac{\mu |\mathbf{b}_t| |\mathbf{b}_r|}{2\pi(1-\nu)} \frac{\sin\theta - \sin 2\gamma \cos\theta}{R}, \quad (21)$$

$$\frac{F_g}{L} = \frac{\mu |\mathbf{b}_t| |\mathbf{b}_r|}{2\pi(1-\nu)} \frac{\cos\theta \cos 2\gamma}{R}, \quad (22)$$

where $\mathbf{b}_{t,r}$ are, respectively, Burgers vectors of test and reference dislocations. If we characterize these forces into the vector notation described by Eq. (13), we can compute the velocity vector and the displacement vector as given by Eqs. (14)–(17).

C. Short-range reactions

Within a distance of several Burgers vectors from the dislocation core, the displacement field around the dislocation is not accurately described by linear elasticity. This dependence breaks down at separation distances less than $R \sim 5b$, hence the region enclosed by this radius is referred to as the dislocation core. Large strains close to

the dislocation core invalidate the assumption of linear elasticity.

In experiments, it is found that many nonlinear processes occur which are describable by a reaction rather than by force-displacement relationships. Nonlinear interactions between dislocations are phenomenologically described as rate processes rather than force-displacement relationships. Some of these nonlinear reactions, or dislocation events, are immobilization of dislocations, annihilation of dislocations, dipole formation, junction formation, and dislocation generation. These nonconservative reactions can be characterized as discrete events, and can therefore accurately represent the phenomena in a controlled computer experiment.

1. Immobilization

If the stress on a mobile dislocation falls below the friction stress, the dislocation becomes immobilized. Once a dislocation is immobilized, the only consequence is that the total vector velocity is identically zero. An immobile dislocation can still contribute its elastic strain energy to the overall computation of internal stress on other dislocations. Immobile dislocations can be remobilized if the effective stress is raised above the friction stress.

2. Annihilation

Annihilation is the cancellation of two dislocations of opposite Burgers vectors which approach each other within a certain critical distance of separation. This annihilation has usually been treated as an average over the crystal of the recovery process.^{18,19} Essmann and Mughrabi²⁰ have estimated a value for the critical distance for annihilation of two screw dislocations of opposite Burgers vectors as

$$y_s \approx \frac{\mu b}{2\pi\tau_g}, \quad (23)$$

where y_s is the annihilation width for screw dislocations and τ_g is the shear stress required for dislocation glide. For copper, $y_s \approx 1.8 \mu\text{m}$; for molybdenum, $y_s \approx 0.19\text{--}2.25 \mu\text{m}$. For mixed or edge dislocations, annihilation will occur when the attractive elastic force between two dislocations exceeds the force required for dislocation climb.²¹ The critical distance for annihilation of mixed dislocations is thus given by

$$y_m = \frac{\mu b^4}{2\pi\kappa U_f \sin\psi}, \quad (24)$$

where y_m is the annihilation width for mixed dislocations, U_f is the energy of formation of atomic defects, ψ is the angle between the Burgers vector and the sense vector of the dislocation, and κ is $1 - \nu < \kappa < \nu$. The critical distance for edge dislocation annihilation has been found to be on the order of 1.6 nm,^{22,23} which is much smaller than the critical distance for screw dislocations. This value is about an order of magnitude less than the average distance between dislocations within the cell bound-

ary. Prinz and co-workers²⁴ determined this value to be greater than 1.6 nm, but their experiments were carried out at higher temperatures than those of Essmann and Mughrabi.²⁰

3. Dipole formation

When two edge dislocations of opposite Burgers vectors approach each other, they can achieve a stable configuration if they remain at a distance greater than the critical distance for annihilation.²⁰ This configuration is known as a dipole and it can exist as a vacancy or interstitial-type configuration. Typical dipole lengths are on the order of tenths of microns.^{20,23} Dipoles are composed only of edge dislocations since screw dislocations can easily annihilate by the cross-slip mechanism. Once formed, a dipole does not move as a whole if the external or internal stresses are changed, but it does change its configuration slightly.²⁵ Application of an applied stress causes a slight change in the relative angle between the dislocations which constitute the dipole.

Two dislocations separated by a sufficient distance to form a dipole will not necessarily form a dipole configuration. It is found^{25,26} that in order to form a stable configuration, the stress on a dislocation must be less than the passing shear stress for a dipole τ_p , i.e.,

$$\tau_p \approx \frac{\mu b}{8\pi(1-\nu)y}, \quad (25)$$

where y is the slip plane spacing.

A dipole does not necessarily represent the perfect alignment of two dislocations of opposite Burgers vectors. In fact, the relative angle between two dislocations in a dipole varies from 25° to 65°,²³ with an average around 45°. The latter angle represents the position of minimum interaction energy of dislocations within a dipole.

4. Junction formation

Attractive dislocations are those dislocations which experience a net attractive force with respect to each other. If the dislocations are parallel, then the difference in Burgers vectors between two attractive dislocations is between 90° and 270°. If two attractive dislocations approach each other, they will eventually intersect each other, the intersection being an annihilation event if the two dislocations are of opposite Burgers vectors. If they are not of opposite Burgers vectors, then one of three events can occur: (1) They lock together, forming a Lomer-Cottrell barrier; (2) they draw each other out, forming a jog intersection; or (3) they intersect and then pass each other. The two dislocations will pass each other if the net stress on one of the dislocations is approximately greater than the pinning stress for dislocations which is given by

$$\sigma_p = \frac{\mu b}{2\pi\lambda_d}, \quad (26)$$

where λ_d is the interdislocation separation distance.

5. Dislocation multiplication

Dislocation multiplication is primarily attributed to the Frank-Read mechanism²⁷ for glide processes. During dislocation creep, the Frank-Read source is dominant and multiplication occurs by pinning of the dislocation, bowing out, and wrapping around the pinning points. Caillard and Martin²⁸ identified these points in aluminum as primarily small precipitates or impurity clusters and, to some degree, junction segments produced by two dislocations.²⁹ The latter mechanism is ruled out by the aforementioned authors as a major source, because the stress necessary to activate sources from these points is usually high enough to cause junction recombination.³⁰ On the other hand, Prinz and Argon³¹ have identified anchoring points as dislocation dipoles and multipole bundles in the evolution of cell-wall-type structures.^{32,33} The bowing out of free segments from these bundles is considered a major generation source.³¹

Multiplication occurs if the total force on a dislocation exceeds the Orowan stress for dislocation reproduction.³⁴ The Orowan stress criterion is given by

$$\sigma_0 = \frac{2\mu b}{\lambda}, \quad (27)$$

where λ is the interobstacle spacing. If this criterion is satisfied, dislocations are capable of multiplying at a rate

$$\dot{\rho} = \rho \frac{v_g}{\lambda}, \quad (28)$$

where ρ is the total dislocation density. Dislocation multiplication is also possible by a process of climb, similar to the Frank-Read source, known as the Bardeen-Herring mechanism.³⁵ This process is dominant under conditions of vacancy supersaturation, such as irradiation or quenching conditions. The contribution to production due to the bowing of dislocation links by climb has been calculated by Nabarro.⁸ It has been determined, however, that this contribution is usually negligible compared to the recovery creep component³⁶ and is therefore not a major source of production of new dislocations.

III. COMPUTER SIMULATION METHODOLOGY

The interaction physics outlined in the previous section have been integrated into a computer code DISLODYN (dislocation dynamics), which simulates the motion of dislocations projected onto a 2D plane. For dislocations on multiple slip systems, the general methodology for long-range forces outlined in Sec. II B 1 is applied. For parallel dislocations, the method outlined in Sec. II B 2 is applied to reduce computation time. The short-range forces are applied in all cases. The following section describes in detail the methodology used in DISLODYN. We describe the dislocation by two sets of vectors (position and velocity) which constitute the minimum information necessary to characterize its existence in 2D space.

A. Simulation sequence

Initially, a random set of dislocations is introduced into the reaction space. The maximum size for this space

is the grain size. The dislocations introduced into the system are all mobile, and are allowed to experience a relaxation phase after introduction into the system. In this phase, there is no stress applied to the system and dislocations are allowed to reach equilibrium, dependent only upon elastic long-range forces already present from the existing configuration. The dislocations then become immobilized upon reaching equilibrium. Once equilibrium is achieved, the dislocations are then subjected to an externally applied stress (monotonic or cyclic depending upon the physical situation) and the simulation proceeds for the desired length of time.

The simulation sequence ensures that the two dislocations with the most potential for interaction (i.e., short-range reactions) are determined first. All long-range forces are then computed statistically. These forces are used in the velocity-stress relationships to determine the velocities of the mobile dislocations. Immobile dislocations are passed over during this calculation. The time step used for the entire system is then computed. If this time step were infinitely short, the simulation would be an exact computation of the trajectories but it would take a large amount of computer time to execute the problem. A time step must be determined which preserves the dynamics of the system but is long enough to reduce computation time. This is the goal of the following section in which the calculated time step is entirely determined by the two dislocations which undergo the factor reaction, thus preventing third- or multiple-body reactions from occurring within the same time step. Once this time step is known, new positions of the dislocations can be calculated and potential for dislocation multiplication can be determined. The following is the computational sequence: (1) Determination of the short-range interactions between pairs of dislocations within the minimum distance of short-range interaction; (2) determination of long-range forces for mobile and immobile dislocations; (3) calculation of an effective stress; (4) evaluation of mobility of dislocations; (5) computation of dislocation velocities; (6) computation of the time step; (7) computation of the new dislocation positions; and (8) computation of dislocation sources.

B. Time scales

1. Vector time steps

The maximum computational time step for the system is limited by the minimum amount of time it would take two dislocations to experience a reaction (collision or annihilation). If we consider two dislocations of arbitrary Burgers vectors approaching each other, the universal vector time step is expressed by

$$\Delta t_u = \min \left[- \frac{|\Delta \mathbf{R}_{ij} \cdot \Delta \mathbf{v}_{ij}|}{|\Delta \mathbf{v}_{ij}|^2} \right], \quad (29)$$

where

$$\Delta \mathbf{R}_{ij} = (\Delta X, \Delta Y, \Delta Z)_{ij} \quad (30)$$

is the difference in the position vector,

$$\Delta \mathbf{v}_{ij} = (\Delta v_x, \Delta v_y, \Delta v_z)_{ij} \quad (31)$$

is the difference in the velocity vector. Positive values of the time step are achieved if the two dislocations are moving relatively towards each other vectorially. The Δ 's signify relative Cartesian positions and velocities between the two dislocations. For dislocations which move in two coordinate directions, this time step represents the time until a collision between the two dislocations occurs. If the dislocations are of like sign, the collision will be a repulsive event. If the two dislocations are of opposite sign, the collision will be either an annihilation, a dipole formation, or a junction event.

For dislocations which only move in one coordinate direction, this time step corresponds to the time to the distance of closest approach. The value of the minimum time is given by

$$\Delta t_{\min} = \frac{1}{|\mathbf{v}_{ij}|} (|\Delta \mathbf{R}_{ij}|^2 |\Delta \mathbf{v}_{ij}|^2 - |\Delta \mathbf{R}_{ij} \cdot \Delta \mathbf{v}_{ij}|^2)^{1/2}. \quad (32)$$

Close inspection reveals that this expression is equivalent to the triangle inequality identity. If the two dislocations are on a collision course, then the discriminant in Eq. (32) for minimum separation is identically equal to zero. If the two dislocations are incapable of short-range interaction, then the value of the discriminant is positive.

Advancement time step. If two approaching dislocations are of opposite Burgers vectors and their interaction limits the system dynamics, then the calculated time step should be the time it takes the dislocations to experience a short-range interaction, not the time it takes for the dislocations to occupy the same space. This advancement vector time step is given by

$$\Delta t_a = \min(\Delta t_u) \left[1 - \left| 1 - \frac{|\Delta \mathbf{v}_{ij}|^2}{|\Delta \mathbf{R}_{ij} \cdot \Delta \mathbf{v}_{ij}|^2} \times (|\Delta \mathbf{R}_{ij}|^2 - \delta_0^2) \right|^{1/2} \right], \quad (33)$$

where δ_0 is the characteristic short-range interaction distance. This is a more stringent time-step requirement than the previous one because the term in the inner square brackets is ≤ 1 . This time step, however, preserves the dynamics of the simulation and allows the short-range interactions to properly proceed from one simulation step to the next.

2. Interactive time steps

(a) *Dynamical time step.* Dissimilar dislocations which determine the time step can be removed from the system upon short-range interaction, thus allowing control of the dynamics to be returned to other components of the system. Similar dislocations can determine the system dynamics until the force between them becomes too large or until stable dislocation patterns form. In either case, the time step should not be fixed on any two dislocations for more than two or three iterations. This condition is satisfied in the DD methodology, and in most cases the time step of two consecutive iterations is determined by two completely different sets of dislocations. This change

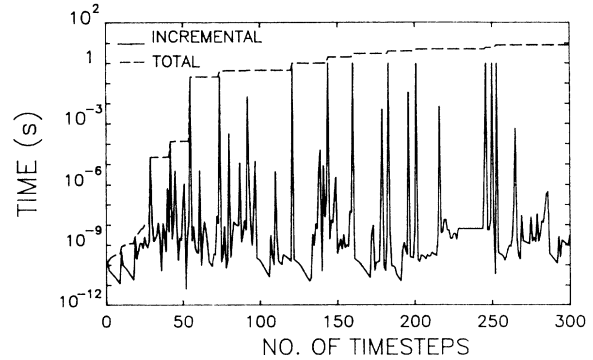


FIG. 3. Dynamic time stepping (copper at 23 °C, 8 cycles, 1 Hz).

in time step from one iterative step to the next is termed dynamic time stepping. Figure 3 is an example of dynamic time stepping for a condition of cyclic straining of copper at 25 °C.

(b) *Equilibrium time step.* If two dislocations have the same Burgers vector sign, they can introduce an additional constraint on the time step. We consider one mobile dislocation constrained to glide motion toward an immobile dislocation. We can represent the equilibrium situation by a plot of the potentials of the dynamic interaction of these two dislocations. The elastic interaction potential for two dislocations in iron is depicted in Fig. 4. An immobile dislocation is placed at the origin and the position of the mobile dislocation is represented by the abscissa. The potentials depicted by the solid lines represent the potential due to the applied constant force and the elastic interaction energy. The vertical line at position 0.374 μm is the equilibrium position of the mobile dislocation for a stress $\sigma = 108 \text{ dyn/cm}^2$. A logarithmic potential with a singularity at the origin represents the $1/R$ interdislocation repulsive force. The dotted line is the sum of the two potentials. It can be seen that a mobile dislocation moving towards the immobile one will essentially fall into a potential well. Accurate dynamic computer simulations must show a smooth approach to equilibrium without unphysical oscillations, as shown in Fig. 5.

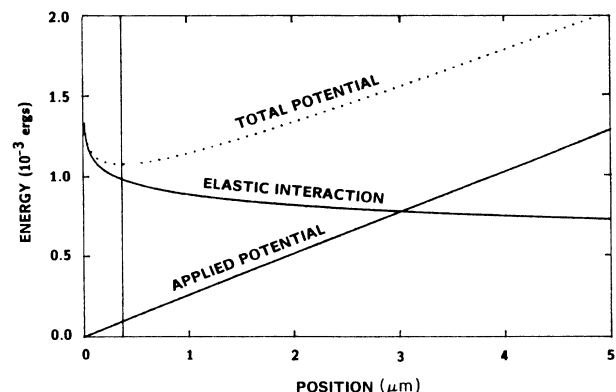


FIG. 4. Potential diagram for 1D motion.

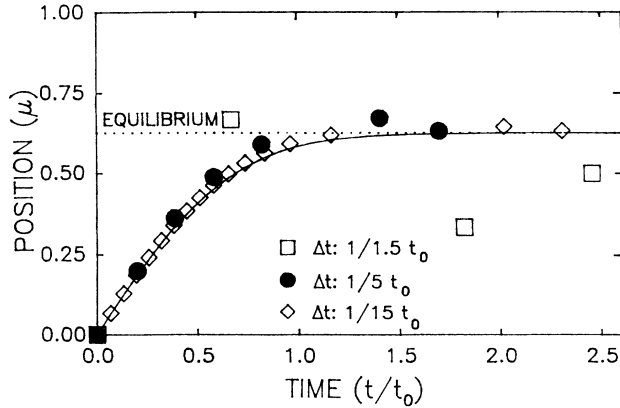


FIG. 5. Dislocation trajectories for 1D motion for various time steps.

The trajectories of a mobile dislocation entering from the bottom toward a locked dislocation at position $1.0 \mu\text{m}$ are shown in Fig. 5. Rotated 90° counterclockwise, this figure corresponds exactly to the first $1\text{-}\mu\text{m}$ block of Fig. 4 (i.e., the dotted horizontal equilibrium line in Fig. 5 corresponds to the solid vertical line in Fig. 4). The scaled time t_0 is the time it would take a dislocation at the origin to arrive at the position of the lock in one time step.

In the case of a dislocation interacting with a lock, we define the equilibrium time step to be a fraction f of Δt_u , i.e.,

$$\Delta t_e = f \Delta t_u . \quad (34)$$

The exact trajectory of the mobile dislocation is represented by the solid line in Fig. 5, and is given by

$$x = x_{\text{eq}} (1 - e^{(\tau_a/A)(x-x_0-v_a t)}) + x_0 e^{(\tau_a/A)(x-x_0-v_a t)} , \quad (35)$$

where $x_{\text{eq}} = x' - (\tau_a/A)$ is the equilibrium dislocation position, x_0 is the initial dislocation position, $A = \mu b / 2\pi(1-\nu)$, v_a is the velocity at the applied stress, and t is elapsed time. The discrete points are applications of the numerical algorithm and time-step criterion [Eq. (34)]. It can be seen from the trajectories that if the time step chosen is too large, the dislocation will occupy a position far away from equilibrium on the following time step and take longer to converge to the equilibrium point. The average relative error in the position of the dislocation is found to be 36% for $f = \frac{1}{1.5}$, 9% for $f = \frac{1}{5}$, and 3% for $f = \frac{1}{15}$. The dynamics of a 1D pileup and details of the numerical scheme for a group of dislocations are given in Ref. 37.

(c) *Multiplication time step.* Multiplication can only occur if the dislocations satisfy the Orowan criterion [Eq. (27)]. The rate of production of dislocations, given by Eq. (28), is based on the average time it takes a dislocation to pass through a set of obstacles and produce dislocation loops. Over long periods of time, many loops are produced from the same dislocation. Equation (28) is approximated by

$$\Delta \rho = \rho \frac{v_g}{\lambda} \Delta t . \quad (36)$$

For multiplication processes, account must be taken of the cumulative time over which multiplication can occur. Therefore, for a given slip strip comprising a number of parallel glide planes within which dislocations have satisfied the Orowan stress criterion, the multiplication time step is limited by the following value:

$$\Delta t_m = \min \left[\frac{N_{\text{loop}}}{\nu' \rho} \right] , \quad (37)$$

where N_{loop} is the maximum number of loops allowed in a given time step and ν' is the frequency of dislocation production and equals v_g/λ .

The time step for each strip is accumulated and the time to production of a new set of loops is computed. Once a strip has experienced dislocation multiplication, its cumulative time step is set to zero. Therefore each strip experiences a different rate of production of dislocations based on its own dislocation density and the force requirements for dislocation multiplication.

3. System time step

The resultant time step for the system is the minimum value of all the previous time steps,

$$\Delta t = \min(\Delta t_u, \Delta t_a, \Delta t_e, \Delta t_m) , \quad (38)$$

and is the value of the time step used in Eq. (15) to evaluate the displacement of each dislocation in the system.

IV. DISCUSSION OF THE DD METHODOLOGY

In conventional MD, the forces on each molecule are computed and an expression for force is inserted into Hamilton's EOM's.¹ In traditional MD, the total energy for a fixed number of atoms in a fixed volume is conserved as the dynamics of the system evolve in time. The dynamical equations are explicitly integrated, yielding particle positions and momenta. Some form of velocity renormalization, or other constraints, are introduced to represent isothermal or isobaric thermodynamic processes.

In standard constant-temperature MD approaches, it is common to monitor the velocities of the particles and apply energy and momentum constraints. This is in accord with the description of a microcanonical ensemble of particles in which the number of particles, the volume, and the total energy are held constant. If the velocities of the particles lead to a deviation in the constant value of temperature above, then the velocities are rescaled until the system reaches equilibrium.

Dislocation dynamics methodology has unique features which are not necessarily embodied in conventional MD. Dislocations represent line defects which interact with each other through a long-range linear elastic field and a short-range nonlinear field. The system size in dislocation dynamics can represent an entire grain, for example, with 10 000 to 100 000 dislocations. In MD, on the other hand, systems containing up to 250 000 particles have

been simulated and are only considered as a statistical sample of matter. Therefore statistical thermodynamical principles can be used to renormalize velocities if the studied phenomenon is near thermodynamic equilibrium. Periodic boundary conditions can be invoked in view of the statistical sampling argument. In DD, the application of thermodynamical concepts and statistical sampling is not yet established. The results of a dynamical simulation of a dislocation system represent a possible and not a sampled behavior of those dislocations contained within a grain. The presence of a long-range vector field for dislocations is not known in the majority of MD simulations where, for example, a Lennard-Jones-type potential is used for spherically symmetric two-body interactions. When short-range dislocation reactions such as annihilation and production are considered, particle conservation principles are not applicable. In MD simulations, particle conservation is a fundamental feature. In a similar way, energy conservation is more difficult to apply because of the various nonconservative dislocation reactions.

It is argued here that such fundamental differences between the DD and MD methodologies are strong enough to differentiate the two simulation approaches. The DD methodology is viewed as a possible new tool for the study of micromechanical problems where dislocations play a significant role. In "Dislocation Dynamics. II." we give several examples of the application of this method to the formation of dislocation patterns.

Several comparisons can be drawn between the methodology used for dislocation systems and those for atomic and molecular systems.

1. Dislocations can glide into an obstacle and eventually become immobilized in their form of a pileup. There is no spatial analogy in molecular systems because molecules are not immobilized in space (even in plasma systems) where, at most, the ions are contained along magnetic field lines.³⁸

2. In molecular systems, all the physics of the molecular simulation is contained in the description of the interatomic potential (e.g., the Lennard-Jones potential^{5,39} or the embedded atom method).⁴⁰

The values of the constants in interatomic potential representations are generally determined through experimental calibration and not from first principles. The forces are calculated from the potential gradient and the accuracy of the forces is completely dependent upon the accuracy of the effective potential in describing the molecular or ionic system.

The forces in dislocation systems, however, are determined from continuum mechanics theory which relies strictly on the distortion of a perfect lattice outside the core of the dislocation. This force is proportional to $1/R$, where R is the distance from the dislocation to the reference point and is known to be exact outside the core radius. This is true for all materials and therefore it is not strictly necessary to compute a potential for the sys-

tem before calculating the forces necessary to execute a physically meaningful simulation. The only other system in which the forces are explicitly known is a plasma system, in which the velocity EOM is calculated explicitly using the Lorentz force.

3. The examples of the interatomic potentials presented here are designed to represent the physics of a two-molecular interaction by a repulsive force up to a critical distance between the molecules. Less than this distance, the potential becomes attractive and therefore large angle collisions between molecules are avoided. The $1/R$ force for dislocation systems, however, does not lend itself to this physical scenario. Dislocations of the same Burgers vector sign cannot overlap, and hence particles of the same sign will forever exert a repulsive force on each other. Because the dislocations have different Burgers vectors, the Burgers vector direction also determines the type of interaction. There is no analogy in molecular systems.

4. There are many short-range effects in DD which do not exist in MD. The formation of immobilized structures in space (i.e., immobile dislocations, dipoles, and junctions) has no analogy in MD. In DD, two opposite particles can annihilate each other, whereas molecules are incapable of doing this. Dislocations are also able to reproduce in dislocation multiplication. No self-reproduction mechanism exists in molecular theory. The closest thing to a short-range effect in MD is a chemical reaction. However, this depends upon direct collision of molecules and these events are usually considered negligible in molecular simulations.

- (5) One final difference between MD and DD simulations is that dislocations are dipolar particles with a vector field while molecules are essentially monopolar particles with no orientation effects. This leads to a more complicated formulation of simulation dynamics in DD than in MD.

In this paper, we have attempted to introduce the DD methodology as a potential computational tool which may allow a study of complex micromechanical deformation phenomena. It is hoped that this method will form a bridge across our knowledge gap between the behavior of single dislocations and their collective influence on the deformation of solids. In our companion paper we give specific applications of the DD method and show that the unique features of the vectorial dislocation elastic-stress field, coupled with the nonlinearity of short-range reactions, do indeed result in observed self-organization phenomena such as persistent slip bands, planar arrays, and dislocation cells.

ACKNOWLEDGMENTS

This work was supported by the U. S. Department of Energy, Office of Fusion Energy, Grant No. DE-FG03-84ER52110, with UCLA.

*Current address: Xerad Inc., 1526 14th Street, Suite 102, Santa Monica, CA 90404.

- ¹B. J. Alder and T. E. Wainwright, *J. Chem. Phys.* **27**, 1208 (1957).
- ²A. Rahman, *Phys. Rev. A* **136**, 405 (1964).
- ³L. Verlet, *Phys. Rev.* **15**, 98 (1967).
- ⁴H. C. Andersen, *J. Chem. Phys.* **72**, 2384 (1980).
- ⁵F. F. Abraham, *Adv. Phys.* **35**, 1 (1986).
- ⁶M. J. Turunen, *Philos. Mag.* **30**, 1033 (1974).
- ⁷P. Ostrom and R. Lagneborg, *J. Eng. Mater. Tech. Trans. ASME, Ser. H* **98**, 114 (1976).
- ⁸F. R. N. Nabarro, *Philos. Mag. A* **16**, 231 (1967).
- ⁹R. Sandstrom, *Acta Metall.* **25**, 905 (1977).
- ¹⁰W. G. Johnston and J. J. Gilman, *J. Appl. Phys.* **33**, 129 (1959).
- ¹¹D. F. Stein and J. R. Low, Jr., *J. Appl. Phys.* **32**, 362 (1960).
- ¹²R. W. Rohde and C. H. Pitt, *J. Appl. Phys.* **38**, 876 (1967).
- ¹³W. F. Greenman, T. Vreeland, Jr., and D. J. Wodds, *J. Appl. Phys.* **38**, 3595 (1967).
- ¹⁴M. A. Meyers and K. K. Chawla, *Mechanical Metallurgy* (Prentice-Hall, Englewood Cliffs, NJ, 1984).
- ¹⁵A. S. Argon, F. Prinz, and W. C. Moffatt, in *Dislocation Creep in Subgrain-Forming Pure Metals and Alloys*, edited by B. Wilshire, and D. R. J. Owen (Pineridge, Swansea, 1981), p. 1.
- ¹⁶M. Peach and J. S. Koehler, *Phys. Rev.* **80**, 436 (1950).
- ¹⁷J. P. Hirth and J. Lothe, *Theory of Dislocations* (Wiley-Interscience, New York, 1982).
- ¹⁸R. Lagneborg, *Met. Sci. J.* **6**, 127 (1972).
- ¹⁹R. Lagneborg, *Met. Sci. J.* **3**, 161 (1969).
- ²⁰U. Essmann and H. Mughrabi, *Philos. Mag.* **40**, 731 (1979).
- ²¹J. Friedel, *Dislocations* (Pergamon, Oxford, 1954).
- ²²U. Essmann and M. Rapp, *Acta Metall.* **21**, 1305 (1973).
- ²³H. Neuhäuser, O. B. Arkan, and H. H. Potthoff, *Mater. Sci. Eng.* **81**, 201 (1986).
- ²⁴F. Prinz, A. S. Argon, and W. C. Moffatt, *Acta Metall.* **30**, 821 (1982).
- ²⁵J. C. M. Li, *Discuss. Faraday Soc.* **38**, 138 (1964).
- ²⁶H. Mughrabi, in *Continuum Models of Discrete Systems*, edited by D. Brulin and R. K. T. Hsieh (North-Holland, Amsterdam, 1981), p. 241.
- ²⁷W. T. Read, *Dislocations in Crystals* (McGraw-Hill, New York, 1953).
- ²⁸D. Caillard and J. L. Martin, *Acta Metall.* **31**, 813 (1983).
- ²⁹D. Caillard and J. L. Martin, in *Creep and Fracture of Engineering and Structures*, edited by B. Wilshire and D. R. J. Owen (Pineridge, Swansea, 1981), p. 17.
- ³⁰G. Saada, *Acta Metall.* **8**, 841 (1960).
- ³¹F. Prinz and A. S. Argon, *Phys. Status Solidi A* **57**, 741 (1980).
- ³²H. Mughrabi, *Philos. Mag.* **23**, 897 (1971).
- ³³A. S. Argon, in *Physics of Strength and Plasticity*, edited by A. S. Argon (MIT Press, Cambridge, 1970), p. 217.
- ³⁴D. Olander, *Natural Technical Information Center Report No. TID-26711-Pl*, 1976.
- ³⁵J. Bardeen and C. Herring, *Imperfections in Nearly Perfect Crystals* (Wiley, New York, 1952).
- ³⁶B. Burton, *Philos. Mag. A* **45**, 657 (1982).
- ³⁷R. Amodeo and N. M. Ghoniem, *Int. J. Eng. Sci.* **27**, 653 (1988).
- ³⁸C. K. Birdsall and A. B. Langdon, *Plasma Physics via Computer Simulation* (McGraw-Hill, New York, 1985).
- ³⁹M. J. L. Sangster and M. Dixon, *Adv. Phys.* **25**, 247 (1976).
- ⁴⁰M. S. Daw and M. I. Baskes, *Phys. Rev. B* **29**, 6443 (1984).